OFDM radar with LTE waveform

OFDM Radar with LTE Waveform: Processing and Performance

Carlos Baquero Barneto[#], Lauri Anttila[#], Marko Fleischer[*], and Mikko Valkama[#]

[#]Tampere University of Technology, Tampere, Finland
[*]Nokia Mobile Networks, Ulm, Germany

***Abstract*— This paper addresses the processing principles and performance of OFDM based radar, with particular focus on the LTE mobile network base-stations and the use of the LTE downlink transmit waveform for radar/sensing purposes. We specifically address the problem stemming from the unused subcarriers, within the transmit signal passband, and their impact on the frequency domain radar processing. We also formulate and adopt a computationally efficient interpolation approach to mitigate the effects of such empty subcarriers in the radar processing. We evaluate the target range and velocity estimation performance through computer simulations, and show that high-quality target detection can be achieved, with LTE waveform, when combined with the interpolation approach. Impacts of the different LTE carrier bandwidths and number of transmitted LTE sub-frames are also evaluated, together with aggregating up to 5 individual 20 MHz LTE carriers.**

***Index Terms*— OFDM, LTE, radar, RF convergence, joint communications and sensing.**

I. Introduction

Many new technologies and applications demand higher and higher communications capacities and bandwidth while the importance of various radio-based sensing schemes is also continuously increasing, covering commercial, industrial and military fields [1]. Good examples where both radio communications and sensing are of high importance are, e.g., autonomous cars and automotive sector overall, flight control systems as well as medical sensors and monitoring [1], [2], [3]. While classically radio communications and radio-based sensing systems are designed, developed and deployed completely independently of each other, the congestion of the available radio spectrum has started to raise interest in merging these functionalities and systems to same frequency bands and potentially even to same hardware platforms. This is commonly referred to as RF convergence in the literature, with comprehensive state-of-the-art survey being available in [1].

The merger or joint operation of communications and radar systems implies that the same waveform is utilized for both tasks. It is generally well known that orthogonal frequency division multiplexing (OFDM) based waveforms are very well suited for radio communications, providing robustness against multi-path fading, facilitating adaptive modulation and coding across subcarriers, as well as offering high flexibility in radio system design and radio resource management. Additionally, the use of OFDM-based waveforms for sensing/radar purposes is raising increasing interest as described, e.g., in [1], [4], [5].

Relatively recently, in [5], a certain level of convergence of mobile communication networks and radar systems was addressed, with a specific focus on the use of the LTE network downlink reference and synchronization signals for passive radar purposes. In this paper, we also focus on LTE mobile network and the use of the corresponding downlink transmit signals for radar/sensing purposes. However, we assume that there is sufficient isolation between the transmitter and the receiver of the eNodeB such that when viewed from the sensing point of view, it can essentially act as a monostatic radar and thus utilize the complete downlink waveform for radar processing. We then deploy frequency domain radar processing, similar to [2], while putting specific emphasis on the exact frequency domain structure of LTE downlink signals over multiple sub-frames, potentially up to a complete radio frame of 10 ms [6]. We also specifically address the impact of null/unused subcarriers, within the transmit signal passband, of various OFDM symbols in the LTE radio frame and develop a time-frequency interpolation type of an approach to reduce their effects in the radar processing.

The rest of the paper is organized as follows: In Section II, the considered OFDM radar system model is described, incorporating the frequency-domain radar processing based on 3GPP LTE specifications compliant transmit waveform. Then, in Section III, simulation results are provided and analyzed to assess the target range and velocity estimation performance. Finally, Section IV concludes the work.

II. OFDM Radar System Model

The radar functionality is pursued in an LTE network base-station unit (eNodeB) by utilizing the known transmit waveform together with frequency-domain radar processing as shown in Fig. 1. The radar processing will detect targets surrounding the eNodeB by using the known samples within the LTE frequency domain resource grid over multiple OFDM symbols, denoted by $\mathbf{G}_{Tx}$. This grid contains frequency-domain samples corresponding to the overall composite transmit waveform, thus comprising all the downlink physical and logical channels as described in [6]. The size of the grid or matrix $\mathbf{G}_{Tx}$ is $S \times R$ where S denotes the number of active sub-carriers while R indicates the number of OFDM symbols considered in the radar processing.

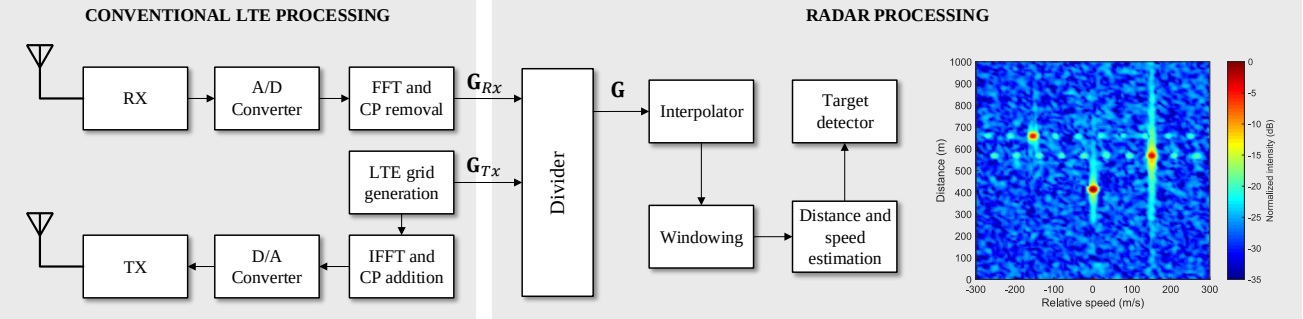

Fig. 1: Block diagram of considered OFDM radar building on conventional LTE downlink waveform and frequency-domain radar processing.

In the transmitter processing, the time domain waveform is generated through block-wise IFFT operating on $\mathbf{G}_{Tx}$, together with cyclic prefix addition, as described in the LTE specifications [6]. The radiated transmit waveform will then interact with one or multiple targets, producing reflections that will be captured by the receiving system. For simplicity, perfect isolation between the transmit and receive systems is assumed in this work, which can in practice be pursued, e.g., through the adoption of separate TX and RX antennas, electrical balance duplexer, active self-interference cancellation, or proper combination thereof. The received signal containing the target reflections is demodulated and processed through FFT to obtain the corresponding receive grid, denoted by $\mathbf{G}_{Rx}$. The distance and the relative speed of a single target correspond to a propagation delay τ_k and a Doppler shift $f_{D,k}$, respectively, relative to the transmit grid $\mathbf{G}_{Tx}$. With K targets or reflected signals, the receive grid sample on pth row and qth column can be expressed as [2]

$$(\mathbf{G}_{Rx})_{p,q} = \sum_{k=0}^{K-1} b_k (\mathbf{G}_{Tx})_{p,q} e^{2\pi j(qT_s f_{D,k} - p\tau_k \Delta f)} + (\mathbf{N})_{p,q} \tag{1}$$

where the samples of the matrix $\mathbf{N}$ correspond to receiver thermal noise, while b_k models the effective attenuation factor of the kth reflection. Furthermore, the sub-carrier spacing and the OFDM symbol duration are denoted by Δf and T_s, respectively. In general, the propagation delay causes a different phase shift for every sub-carrier which can be used to estimate the range of each target. Similarly, the Doppler shift produces a phase shift for the different OFDM symbols that can be utilized to compute the relative speed of the targets.

The actual radar processing is based on the comparison between the transmit and receive grid samples, in order to estimate the range and relative speed of each target. To facilitate this, a new matrix $\mathbf{G}$ is defined with the corresponding samples being calculated as

$$(\mathbf{G})_{p,q} = \frac{(\mathbf{G}_{Rx})_{p,q}}{(\mathbf{G}_{Tx})_{p,q}} = \sum_{k=0}^{K-1} b_k e^{2\pi j(qT_s f_{D,k} - p\tau_k \Delta f)} + (\mathbf{N'})_{p,q} \tag{2}$$

For fixed p and varying q, the above samples correspond to a sum of complex exponentials with oscillating frequencies being defined by the Doppler shifts, thus forming the basis for velocity estimation. Similarly, if q is fixed while p varies, we again obtain a sum of complex exponentials but now the frequencies are defined by the propagation delays which thus facilitates range estimation. However, the LTE transmit grid contains unused subcarriers within the transmit signal passband, whose locations also vary from OFDM symbol to another [6]. Thus, the direct calculation of (2) is not feasible in those points. Therefore, the proposed LTE radar processing includes an interpolation block which deals with these missing samples, along both dimensions p and q where applicable. For computational simplicity, linear interpolation is adopted. After the interpolation stage, the range and relative speed are estimated through estimating the oscillating frequencies of the ratio series in (2), utilizing the interpolated grid which is denoted by $\tilde{\mathbf{G}}$, interpreted as a function of p and q.

As described in [7], the maximum likelihood estimator (MLE) for τ and f_D is the one that maximizes the expression

$$A(s,r) = \left| \sum_{p=0}^{S'-1} \left(\sum_{q=0}^{R'-1} (\tilde{\mathbf{G}})_{p,q} (\mathbf{W})_{p,q} e^{-j2\pi \frac{qr}{R'}} \right) e^{j2\pi \frac{ps}{S'}} \right| \tag{3}$$

Notice that in (3), the samples of the interpolated grid $\tilde{\mathbf{G}}$ are first subject to an FFT of size R' on every column, while the result is then subject to an additional FFT of size S' on every row. Both operations should have a size higher than the basic grid dimensions, i.e., $R' \geq R$ and $S' \geq S$. Equation (3) includes also an additional matrix $\mathbf{W}$ which corresponds to windowing of the interpolated grid $\tilde{\mathbf{G}}$. In radar applications, the main advantage of applying window functions is the ability to control the side-lobe levels [7]. Finally, an actual target detector is used in order to find the maximum or maxima of the expression (3) and compare it or them to the chosen detection threshold. The range and relative speed of each detected target are thereon obtained. We note that the periodogram based approach in (3) is only one feasible approach to create test statistics for target detection, while alternative methods can also be pursued.

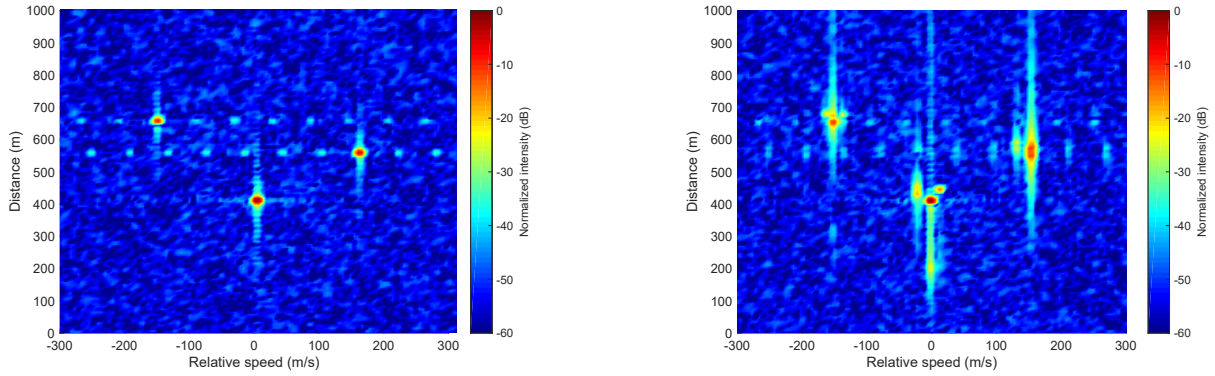

(a) (b)

Fig. 2: Examples of periodogram-based radar images with LTE waveform (20 MHz carrier bandwidth, SNR = 10 dB) and three targets for (a) free space model scenario, and (b) more realistic scenario with multipath propagation.

III. Results and Analysis

Simulations are carried out to evaluate the performance of the LTE waveform based OFDM radar described in Section II. In the evaluations, LTE carrier bandwidths of 3, 10 and 20 MHz are considered, corresponding to LTE resource grids with 15, 50 and 100 resource blocks (RBs), respectively. The assumed LTE network center-frequency is 2.6 GHz, and all the main downlink physical channels and signals (PSS, SSS, CRS, PDSCH, PDCCH, PCFICH, PHICH, PBCH) are modelled. For simplicity, R' and S' are set to R and S, respectively. Basic Hamming window is used as the window function in (3). Additionally, we also study the performance when aggregating 5 individual 20 MHz LTE channels through carrier aggregation (CA).

First, Fig. 2 presents a representative example of the obtained radar images in a scenario with 3 different targets subject to different propagation conditions, while assuming 20 MHz carrier bandwidth. Fig. 2a) illustrates a radar image with a propagation environment building on the basic free space path loss. In this ideal scenario, the peaks presented in the radar image are determined by the oscillating frequencies of the ratio series in (2), which in turn are defined by the Doppler shifts and propagation delays of the different targets. However, in most of the cases in reality, the propagation environment contains multipath effects [8]. When multipath occurs in radar systems, the RX antenna collects the direct reflection of the targets combined with other indirect reflected and/or scattered waves which cause virtual targets as illustrated in Fig. 2b). Accordingly, we assume this more realistic multipath environment case in the following evaluations.

To evaluate the performance of the considered system more extensively, we first analyze the specific scenario in terms of the target distances and velocities presented in Fig. 2b). Considering a complete LTE radio frame of 10 ms and 20 MHz carrier bandwidth, the TX grid consist of S = 1200 active sub-carriers and R = 140 OFDM symbols

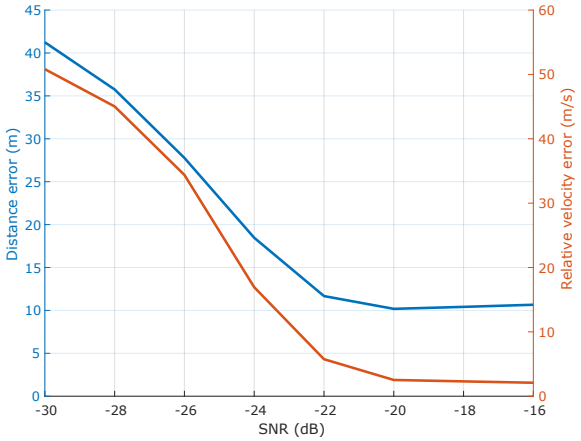

Fig. 3: Target distance and velocity estimation error results for varying received SNR in a scenario with three true targets together with multipath propagation as shown in Fig. 2b).

[6]. Consequently, Fig. 3) shows the achievable distance and velocity estimation errors as functions of the receiver SNR. Clearly, very accurate estimation can be obtained down to -20 dB SNR.

Next, we pursue further performance evaluations by varying the key parameters S and R, which directly depend on the LTE carrier bandwidth and the amount of LTE subframes used for radar processing, respectively. We also now vary randomly the distances (uniformly distributed, within 400 to 800 m) and relative speeds (uniformly distributed, within -200 and 200 m/s) of the involved targets, while also study the impacts of the receiver SNR. Fig. 4a) presents the obtained estimation error behavior for varying SNR when the target distances and velocities are randomly varied, as described above, for three different carrier bandwidths of 3 MHz, 10 MHz and 20 MHz, when a complete radio frame of 10 subframes is used. As can be observed, the averaged results show a significant improvement in the distance estimation when the number of RBs used in the radar

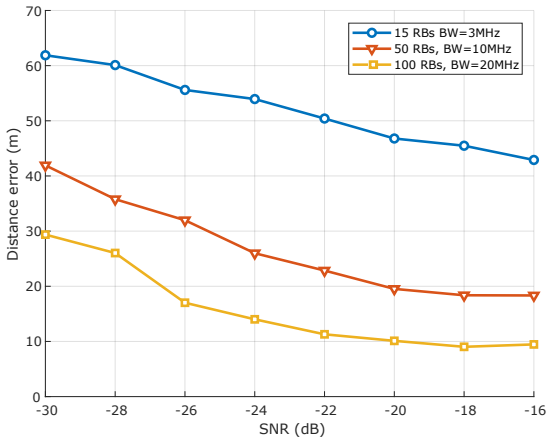

(a)

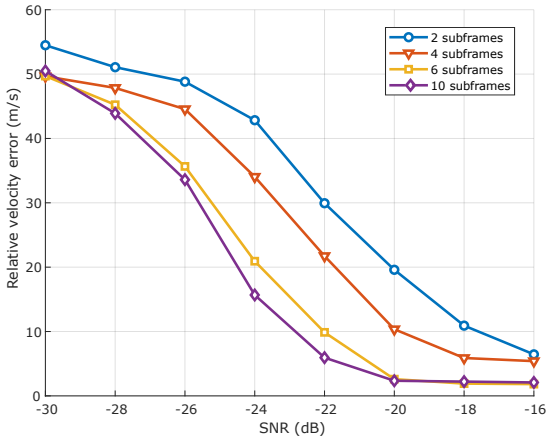

(b)

Fig. 4: Target distance and velocity estimation error results for randomized target scenario with different numbers of (a) LTE carrier bandwidths, (b) LTE subframes used for radar processing. In (a), 10 sub-frames are used while in (b) the carrier bandwidth is 20 MHz.

processing is increased. Similarly, we analyze the effect of the parameter R on the velocity estimation accuracy by varying the amount of the processed LTE subframes, from 2 to 10, for a fixed bandwidth of 100 RBs. As illustrated in Fig. 4b), the velocity estimation error is decreased when number of LTE subframes is increased. Therefore, the best radar performance is achieved when a complete radio frame of 10 LTE subframes with 100 RBs is used.

Finally, we push the bandwidth further and assume that 5 LTE carriers each with 20 MHz carrier bandwidth, can be aggregated and processed. While LTE specifications basically allow for versatile non-contiguous intraband and interband CA schemes, we assume contiguous aggregation of neighboring carriers for simplicity. The corresponding results in terms of the distance and velocity estimation accuracy, shown in Fig. 5, present a significant improvement over the basic 20 MHz carrier case.

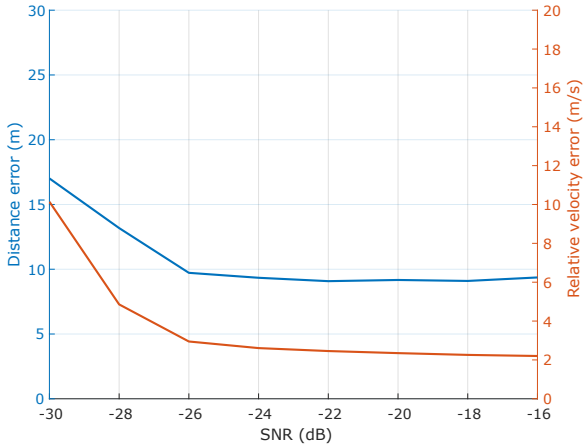

Fig. 5: Target distance and velocity estimation error results in randomized target scenario when aggregating five 20 MHz LTE carriers.

IV. Conclusion

In this paper, the use of LTE downlink waveform for radar/sensing purposes was addressed and studied. Frequency-domain radar processing building on the LTE time-frequency resource grid, complemented with interpolation to account for missing samples due to the null subcarriers within the transmit waveform passband, was described. The target range and velocity estimation performance of the considered method were evaluated numerically, demonstrating that high-quality target detection can be achieved.

Acknowledgment

This work was partially supported by the Academy of Finland (grants #288670 and #301820), Nokia Bell Labs, Finland, and the Doctoral School of Tampere University of Technology, Finland.

References

[1] B. Paul, A. R. Chiriyath, and D. W. Bliss, "Survey of RF communications and sensing convergence research," *IEEE Access*, vol. 5, pp. 252–270, 2017.

[2] M. Braun, "OFDM radar algorithms in mobile communication networks," Ph.D. dissertation, Karlsruhe Institute of Technology, 2014.

[3] Y. L. Sit, C. Sturm, and T. Zwick, "Doppler estimation in an ofdm joint radar and communication system," in *2011 German Microwave Conference*, March 2011, pp. 1–4.

[4] C. Sturm, T. Zwick, and W. Wiesbeck, "An OFDM system concept for joint radar and communications operations," in *VTC Spring 2009 - IEEE 69th Vehicular Technology Conference*, April 2009, pp. 1–5.

[5] A. Evers and J. A. Jackson, "Analysis of an LTE waveform for radar applications," in *2014 IEEE Radar Conference*, May 2014, pp. 0200–0205.

[6] "3GPP TS 36.104 v15.3.0, "Evolved Universal Terrestrial Radio Access (E-UTRA); Base Station (BS) radio transmission and reception", Tech. Spec. Group Radio Access Network, Rel. 15," June 2018.

[7] M. Braun, C. Sturm, and F. K. Jondral, "Maximum likelihood speed and distance estimation for OFDM radar," in *2010 IEEE Radar Conference*, May 2010, pp. 256–261.

[8] Y. L. Sit, L. Reichardt, C. Sturm, and T. Zwick, "Extension of the ofdm joint radar-communication system for a multipath, multiuser scenario," in *2011 IEEE RadarCon (RADAR)*, May 2011, pp. 718–723.